Parameter Study and Design of Wide-Band Widescan Dual-Polarized Tapered Slot Antenna Arrays

Tan-Huat Chio and Daniel H. Schaubert, *Fellow, IEEE*

***Abstract*—A parameter study of dual-polarized tapered slot antenna (TSA) arrays shows the key features that affect the wide-band and widescan performance of these arrays. The overall performance can be optimized by judiciously choosing a combination of parameters. In particular, it is found that smaller circular slot cavities terminating the bilateral slotline improve the performance near the low end of the operating band, especially when scanning in the H-plane. The opening rate of the tapered slotline mainly determines the mid-band performance and it is possible to choose an opening rate to obtain balanced overall performance in the mid-band. Longer tapered slotline is shown to increase the bandwidth, especially in the lower end of the operating band. Finally, it is shown that the H-plane anomalies are affected by the array element spacing. A design example demonstrates that the results from the parameter study can be used to design a dual-polarized TSA array with about 4.5 : 1 bandwidth for a scan volume of not less than $\theta = 45^\circ$ from broadside in all planes.**

***Index Terms*—Antenna arrays, broad-band antennas, slot antennas.**

I. Introduction

THE stripline-fed tapered slot antenna (TSA) array was introduced by Lewis *et al.* [1] in 1974. Its potential for wide-band and widescan arrays makes it a prime candidate for high-performance phased-array systems. However, achieving a successful design is usually costly and time consuming since the relationships between antenna parameters and array performance are not well understood. This is especially true in designing phased arrays since mutual coupling between the antenna elements is significant in determining the ultimate performance. This paper attempts to aid array designers and system engineers to design TSA arrays by providing information about achievable performance and relationships between specific array parameters and performance. These results should improve confidence in proposed array designs and reduce the numerical and empirical iterations needed to optimize arrays for particular applications.

Some recent papers presented studies [2], [3] on single-polarized TSA arrays and identified some of the relationships between design parameters and array performance. These papers use a full-wave method of moments (MoM) analysis that has been extensively verified by comparison to experiments and to other numerical analyses. Recently, Wunsch [4] presented a full-wave Green's function-MoM analysis program that is capable of analyzing dual-polarized infinite TSA arrays. A typical array is shown in Fig. 1.

Dual-polarized arrays have the advantage of polarization diversity. This is especially important in radar and remote sensing applications, which often require the system to transmit and receive multiple and/or arbitrary polarizations. As such, dual-polarized TSA arrays are more versatile than single-polarized TSA arrays but analyzing them is more involved and difficult. A design that has good performance in both polarizations for all scan angles of interest may also be more difficult to achieve.

Designing a wide-band scanning array is also difficult. Typically, the element spacing should be less than one-half free-space wavelength of the highest frequency to avoid grating lobes. In the case of a 5 : 1 bandwidth array, the array element spacing may be less than one-tenth of the free-space wavelength at the lowest frequency. Mutual coupling between the radiating elements may be quite large and this coupling may cause scan-blindnesses and/or anomalies within the desired bandwidth and scan volume. Furthermore, the physics that governs the TSA array is not well known and reliable, simple models are not available. Therefore, in the absence of computer generated design data, a large number of prototype arrays must be constructed since the dual-polarized nature of the array is not amenable to waveguide simulator studies.

A suitable alternative to the time consuming and expensive task of constructing prototype arrays is to make use of full-wave numerical methods to study these arrays extensively. Other than the Green's function-MoM method mentioned previously, the finite-difference time-domain (FDTD) method [5] and the finite-element method (FEM) [6]–[8] may also be used to analyze dual-polarized TSA arrays. Finite domain methods are inherently CPU intensive and require a lot of memory especially if there are thin stratified layers within the unit cell. FEM that use tetrahedra are more amenable to subtle structural changes. FDTD may be more restrictive since rectangular bricks are commonly used, but the FDTD method is very efficient for analyzing wide-band structures since wide-band frequency domain data are easily computed via the fast Fourier transform (FFT) of the time domain results [5]. The Green's function-MoM analysis, although computationally intensive, is suitable for analyzing structures with thin stratified layers since they are taken into account in the Green's functions. In this paper, a Green's function-MoM analysis program that can provide reasonably accurate and reliable results in an acceptable amount of time is used.

In order to further reduce the amount of time taken to perform the parameter study of a dual-polarized TSA array, the

Manuscript received May 20, 1999; revised March 8, 2000. This work was supported in part by The Netherlands Foundation for Research in Astronomy (NFRA).

The authors are with the Department of Electrical and Computer Engineering, University of Massachusetts at Amherst, Amherst, MA 01003 USA (email: schaubert@ecs.umass.edu).

Publisher Item Identifier S 0018-926X(00)05802-6.

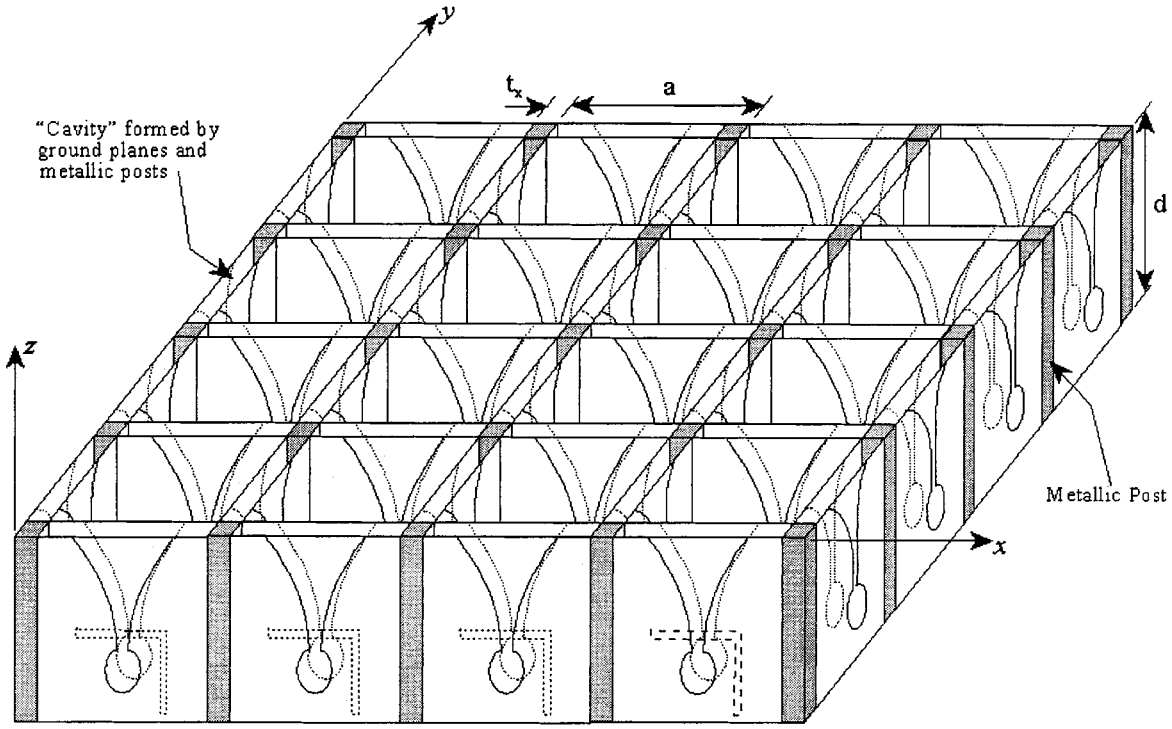

Fig. 1. A dual-polarized TSA array. Elements are separated by metallic posts and the array is backed by metallic ground plane at $z = -d$.

MoM code in [4] has been extended to include frequency interpolation of the impedance matrix [9]. The frequency interpolation method is chosen because interpolation of the impedance matrix in the MoM formulation reliably captures narrowband anomalies like scan-blindnesses. Using the "extended" code, a preliminary study [10] has determined the effects of varying a single parameter of the dual-polarized TSA array at broadside, E-, H- and diagonal- (D-) plane scans in the desired frequency band. In this paper, the study is expanded significantly and culminates in a design example.

With a parameter study like the one presented here, a designer can choose from various cause-and-effect relationships to obtain the desired change in an array's performance. It has been found that the main limitations of the dual-polarized arrays are deteriorating performance in the H-plane as the array is being scanned away from the broadside direction and H-plane anomalies.

The next section describes the antenna structure and the parameters that are studied in detail. Section III presents and discusses the results. A design example with about $4.5:1$ bandwidth and a scan volume of not less than 45° in all planes is given toward the end of the section.

II. Antenna Design Parameters and Method of Analysis

The basic TSA structure used in this study was proposed in [1] although some of its features have been slightly modified to improve performance in [2], [3]. The stripline feed is coupled to bilateral slotline in the ground planes. The bilateral slotline is terminated at one end with a circular slot cavity and at the other end it opens into an exponentially tapered slotline with an opening rate of R, which is defined below. The stripline feed is terminated in a radial line stub. The circular slot cavity and the radial line stub are chosen to terminate the bilateral slotline and stripline feed, respectively, because in [2] and [3] they work well for the single-polarized TSA array and are found to work well for the dual-polarized TSA arrays, too. Therefore, the parameters in [2] and [3] are taken to be the basis for the study here. Fig. 1 depicts a dual-polarized array while Fig. 2 shows the details of one face of the TSA element. In this study, the scan input impedance of an "active" TSA element $Z_{\text{in}} = R_{\text{in}} + jX_{\text{in}}$ in a large (infinite) array environment, obtained from the MoM solution based on the formulation in [4], is shown.

Some of the parameters, like the shape of the slot cavity, the shape of the stripline-feed termination, substrate thickness, and the stripline-slotline transition have been studied in moderate detail in [2]. Furthermore, the stripline stub was found to contribute a series reactance to the overall scan input impedance. This reactance is independent of the other antenna parameters so the radial line stub can be accounted for by using a simple equivalent circuit and need not be included in the MoM analysis. These findings are also valid for the current dual-polarized TSA array structure and are not repeated in this paper. The present study will also take advantage of the results for single-polarized arrays as a starting point to create a baseline configuration antenna here.

The baseline antenna structure is shown in Fig. 2 and has "fixed" parameters as follows: the substrate is $t = 0.288$ cm thick with $\varepsilon_r = 2.2$, the slotline is 0.1 cm wide and 0.5 cm long terminated with circular cavity at one end, the stripline is 0.1 cm wide, and has a characteristic impedance $Z_c = 81\ \Omega$, the stripline terminates in a radial line stub 0.8 cm long and a flare angle of 80°, the backwall offset from slotline cavity is 0.5 cm

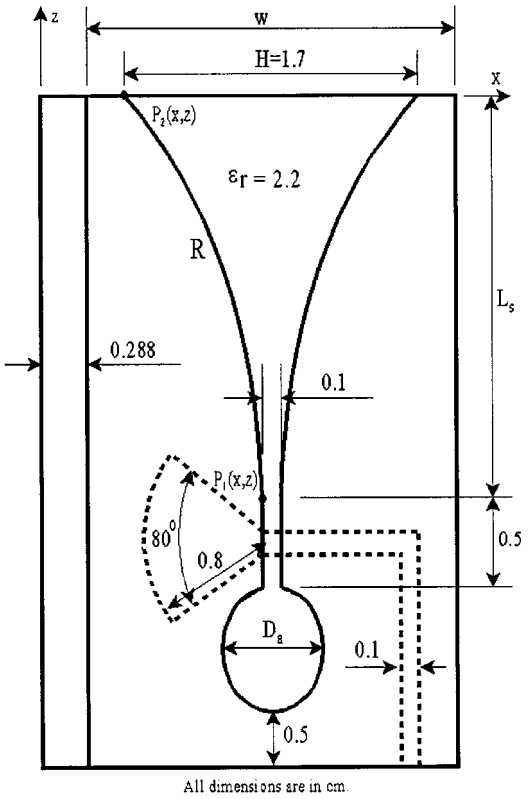

Fig. 2. Typical element configuration. Effects of parameters L_s, D_a, R and w are studied in this paper.

and the tapered slotline width at the radiating aperture plane is $H = 1.7$ cm. The array element spacing is $a = 2.288$ cm in both the x- and y-directions. The parameters to be investigated in this paper are: 1) diameter of the circular slotline cavity D_a; 2) exponential opening rate R; 3) length of the tapered slotline of the antenna element L_s; and 4) element width, $w = a - t$. The exponential curve in Fig. 2 is defined by $P_1(z_1, x_1)$ and $P_2(z_2, x_2)$ (dimensions in centimeters) according to

$$x = c_1 e^{Rz} + c_2 \tag{1}$$

where

$$c_1 = \frac{x_2 - x_1}{e^{Rz_2} - e^{Rz_1}} \tag{2}$$

$$c_2 = \frac{x_1 e^{Rz_2} - x_2 e^{Rz_1}}{e^{Rz_2} - e^{Rz_1}}. \tag{3}$$

Lossy materials are not used in this study, so the radiation efficiency is high.

III. Results, Discussion, and Design Example

With all but one of the above parameters fixed Z_{in} is computed at frequencies from 0.8–7.2 GHz at 0.4 GHz intervals and scan angles in the E-, H-, and D-planes from broadside to $\theta = 45°$. Frequency interpolation fills in values of Z_{in} between the 0.4-GHz steps. Small discontinuities sometimes appear in the plots at the boundaries of the interpolation intervals, e.g., see 1.4 and 1.8 GHz in Fig. 4(b). These could be smoothed, but are left as computed to indicate regions where the interpolation may be less accurate. The reference plane for impedance computations is the stripline-slotline transition and the voltage standing wave ratio (VSWR) is computed with respect to the characteristic impedance $Z_c = 81\ \Omega$ of the stripline feed.

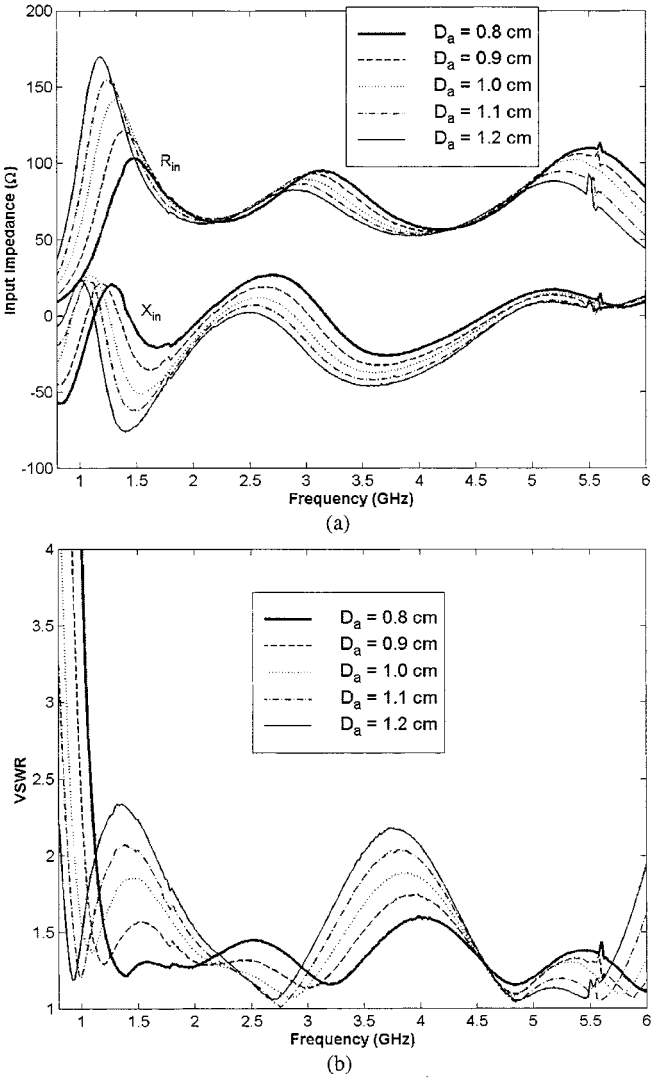

Fig. 3. Effects of slotline cavity diameter at broadside scan on (a) scan input impedance and (b) VSWR.

A. Diameter of the Circular Slotline Cavity D_a

The effects of the circular slotline cavity are studied with the other parameters fixed at $R = 0.3$ cm^{-1}, $L_s = 4.5$ cm and $w = 2.0$ cm. The diameter D_a of the slotline is varied from 0.8 to 1.2 cm and the results are plotted in Figs. 3–6, which show the performance at broadside, E-, H-, and D-plane scans, respectively. Part (a) of each figure shows the scan input impedance while part (b) shows the VSWR with respect the characteristic impedance $Z_c = 81\ \Omega$. At broadside (Fig. 3), the low operating frequency end (f_L) is mainly limited by a rapid decrease in the input resistance. By increasing D_a, f_L improves at the expense of two in-band humps in the VSWR plots around 1.5 GHz and 4 GHz. These are due to the large swings in the resistance and reactance for larger D_a near 1.5 GHz and larger values of negative reactance near 4 GHz. Anomalies sometimes appear near 5.5 GHz in the broadside and E-plane scans (Figs. 3, 5, and 7,

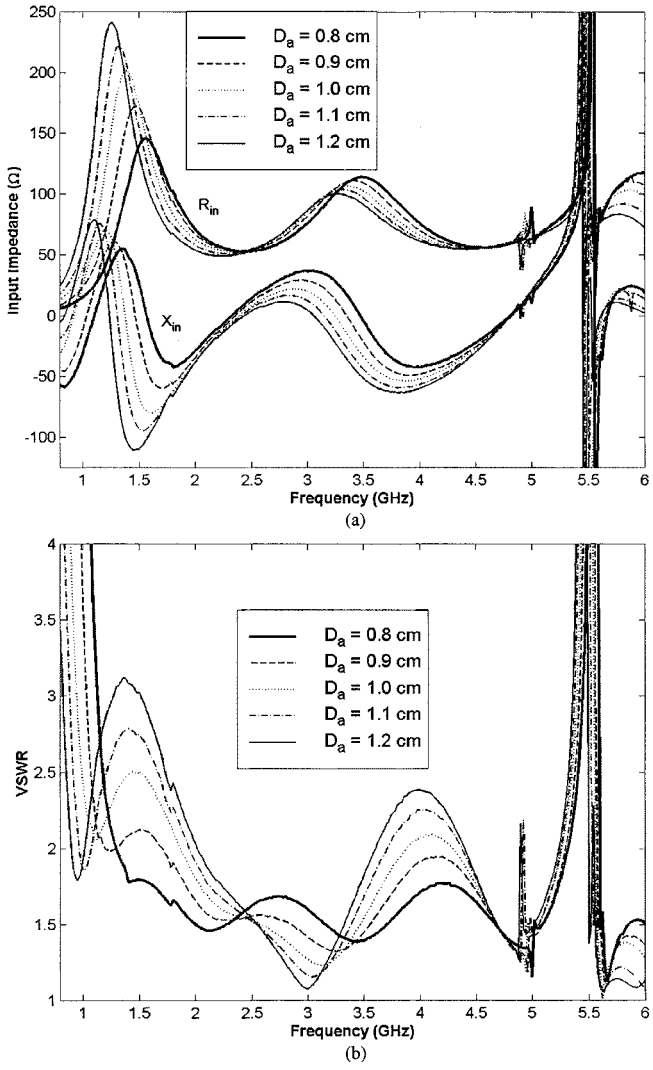

Fig. 4. Effects of slotline cavity diameter at H-plane scan $\theta = 45°$ on (a) scan input impedance and (b) VSWR.

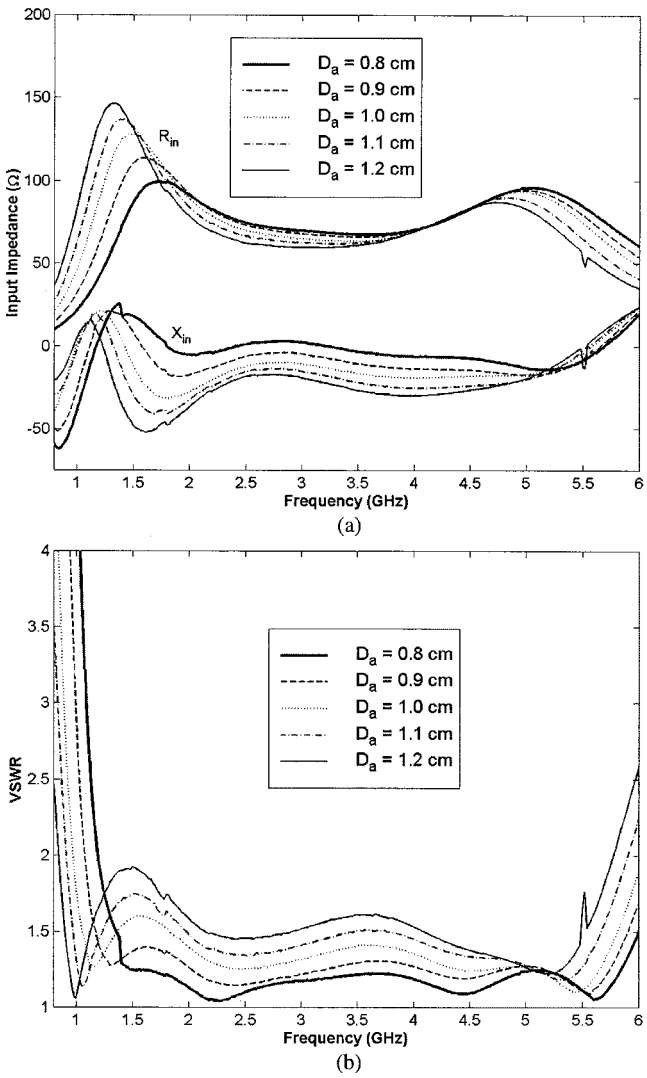

Fig. 5. Effects of slotline cavity diameter at E-plane scan $\theta = 45°$ on (a) scan input impedance and (b) VSWR.

for example). These anomalies are very narrow-band resonances that require small frequency intervals to capture. The frequency intervals used in this study are not sufficiently small to locate these resonances in all cases. These narrow-band anomalies are studied in [11].

Figs. 4 and 5 show results for H- and E-plane, $\theta = 45°$, respectively. As the array is scanned off broadside, the trend observed at broadside remains essentially the same. However, E-plane VSWR generally improves while the H-plane VSWR deteriorates as the array is scanned away from broadside. Furthermore, H-plane anomalies, attributed to cavity modes [4], [11], appear at around 4.9 GHz and 5.5 GHz. The H-plane anomalies are the main limitations of the array at the upper end of the frequency band f_U and will be discussed in more detail in Section III-D. Although not shown here, the anomaly generally exhibits narrower bandwidth at small scan angles than at large scan angles.

Fig. 6 shows the D-plane scan input impedance and VSWR at $\theta = 45°$ beam angle. The scan input impedance is somewhat like a simple average between that of the E- and H-plane impedances. The D-plane exhibits anomalies at exactly the frequencies where the H-plane anomalies occur but the severity is somewhat less. The scan input impedance has been calculated at other scan planes between the E- and H-planes and at each value of θ, the impedance in various planes is approximately a weighted average of the E- and H-plane impedances. In other words, since the H-plane has the worst performance and the E-plane is the best, the performance in the other scan planes is bounded by the performance in the E- and H-planes. This observation is true for all cases presented in this paper. As θ increases, the impedance plots change gradually from the curves at broadside to those at $\theta = 45°$.

B. Opening Rate R

The opening rate R, of the tapered slotline is found to affect mainly the mid-band performance of the TSA array. In this section, R is varied from 0.15 cm^{-1} to 0.6 cm^{-1} while $L_s = 4.5$ cm, $D_a = 1.0$ cm, and $w = 2.0$ cm. The scan input impedances for broadside beam angle are shown in Fig. 7. Varying R does not affect f_L and f_U at broadside very much. However, a larger R causes both the input resistance and reactance

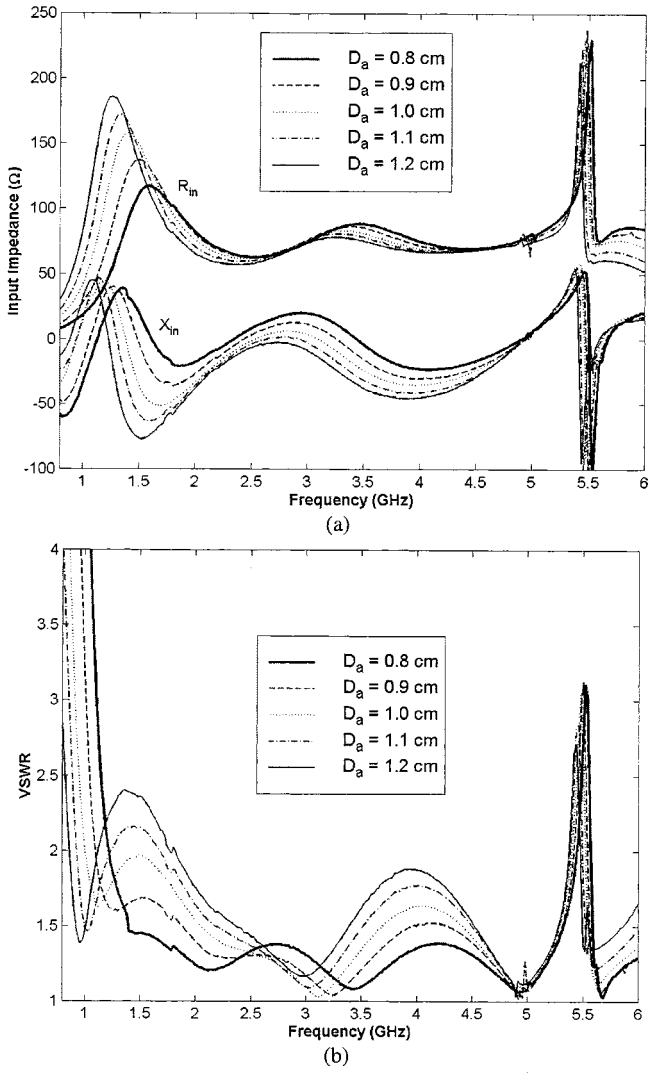

Fig. 6. Effects of slotline cavity diameter at D-plane scan $\theta = 45°$ on (a) scan input impedance and (b) VSWR.

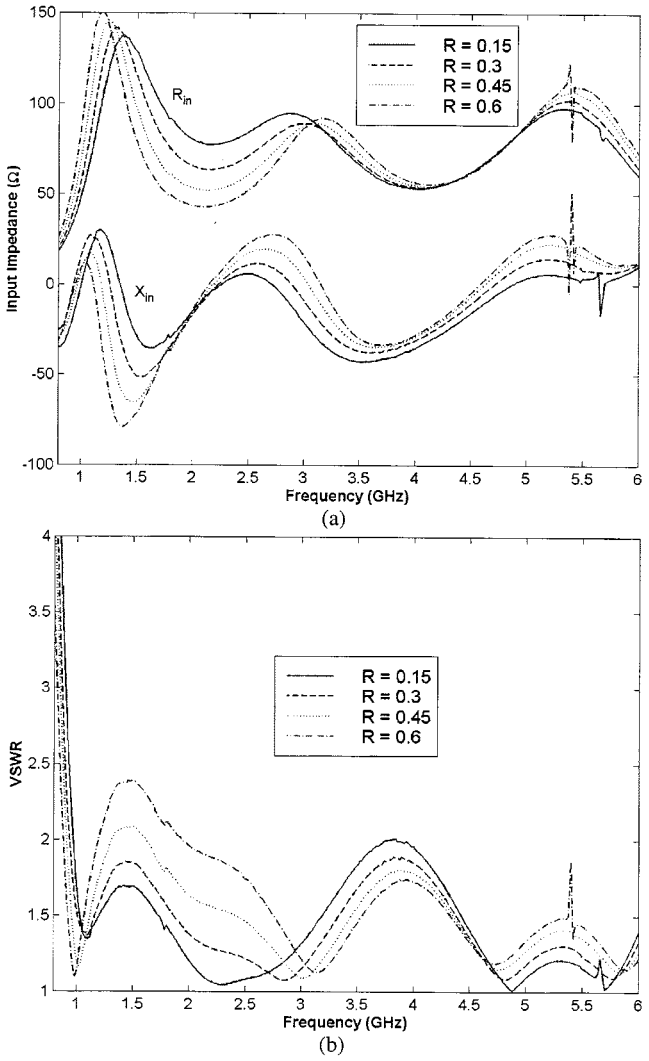

Fig. 7. Effects of opening rate R at broadside scan on (a) scan input impedance and (b) VSWR.

to change more sharply between 1.2–3.0 GHz, which results in a large in-band hump in the VSWR plot with the maximum at around 1.5 GHz. These impedance swings are less severe above 3.0 GHz so the performance is slightly better from 3.0 to 4.5 GHz. On the other hand, a smaller value of R gives larger values of negative reactances in the 3.0–4.5 GHz band, which results in larger VSWR. Therefore, reducing R yields better performance between 1.2–3.0 GHz at the expense of the 3.0–4.5 GHz band.

The impedances for scans at $\theta = 45°$ in the H- and E-planes are shown in Figs. 8 and 9, respectively. As in the other cases, when the antenna is scanned off broadside, the performance improves in the E-plane while it degrades in the H-plane. In Fig. 8, the trend in the H-plane is similar to that observed at broadside, although H-plane anomalies are seen at around 5.0 GHz and 5.5 GHz, respectively. In the E-plane, scan resistances and reactances are somewhat dependent on R, but the net effect on VSWR is relatively small. As for variations of D_a, scan impedances in the intercardinal scan planes are approximately weighted averages of the E- and H-plane values so these results are not shown here.

C. Length of Tapered Slotline L_s

In this section, the effects of the tapered slotline length are studied while the other parameters are fixed at $R = 0.3$ cm^{-1}, $D_a = 1.0$ cm, and $w = 2.0$ cm. It is found that lengthening the tapered slotline improves the f_L performance significantly. Fig. 10(a) shows the input impedances of the various slotline lengths for broadside beam angle. For longer tapered slotlines, the fluctuations of both the resistance and reactance at the low end of the operating band are reduced significantly, which reduces the in-band hump in VSWR near 1.5 GHz (Fig. 10(b)). Furthermore, longer tapered slotlines create larger values of scan input resistance at low frequencies, which also improves the f_L performance. This trend is also observed for E-, H-, and D-plane scans.

Longer tapered slotlines provide better performance, but beyond a certain length the trouble in fabricating such a long antenna may not justify the improvement. Long antennas are more difficult to fabricate because good electrical contact between adjacent elements is essential, which requires that solder or other conducting medium be applied to all corners of the deep and

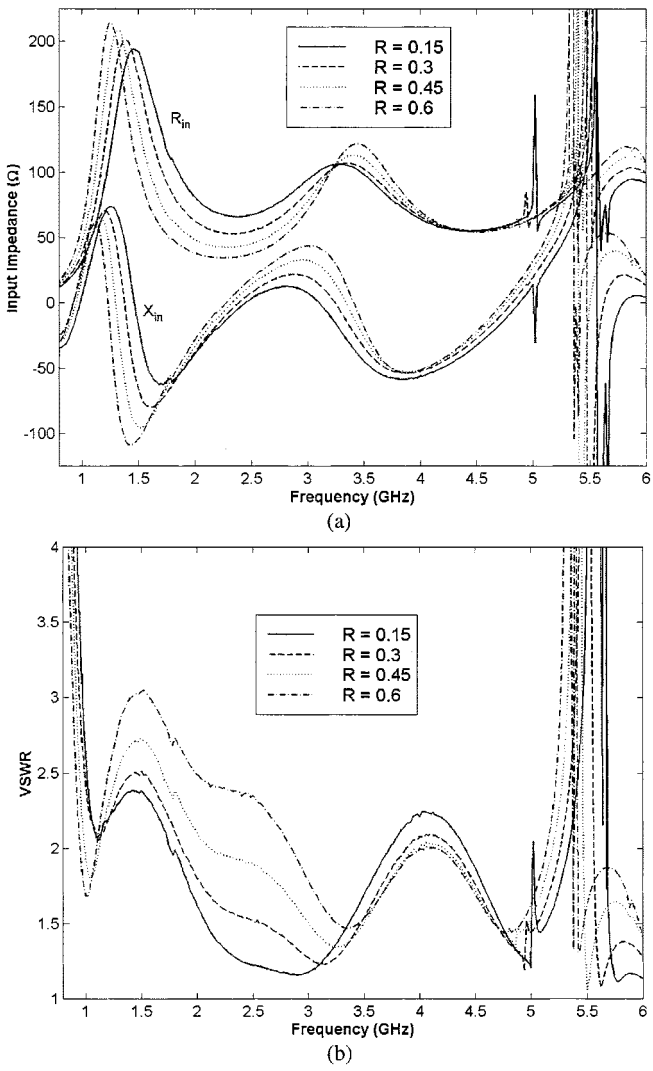

Fig. 8. Effects of opening rate R at H-plane scan $\theta = 45^\circ$ on (a) scan input impedance and (b) VSWR.

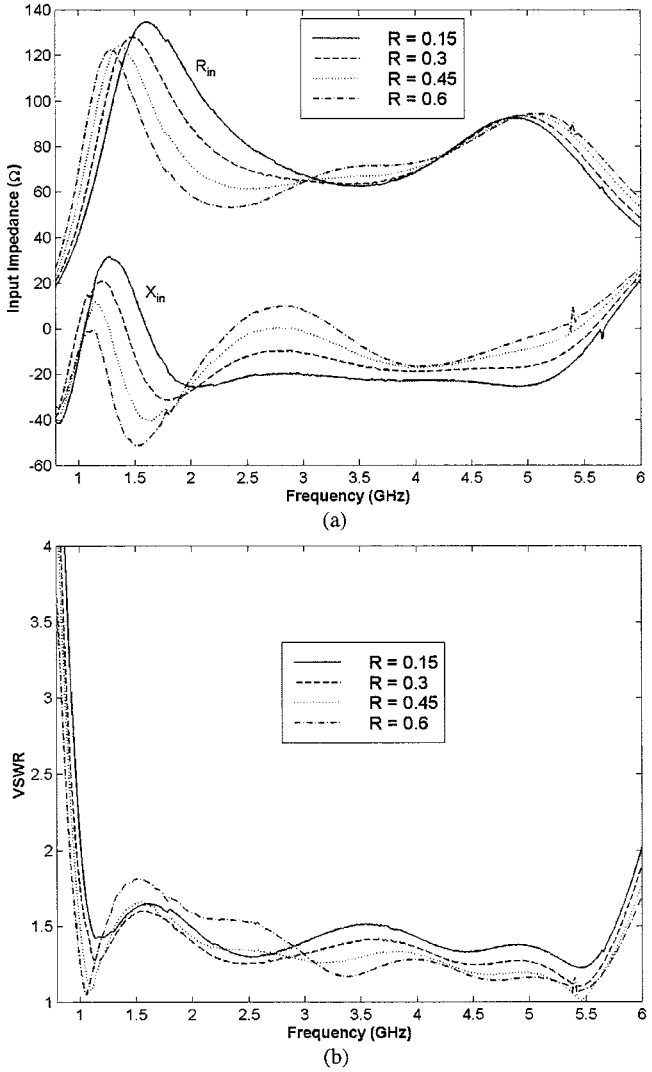

Fig. 9. Effects of opening rate R at E-plane scan $\theta = 45^\circ$ on (a) scan input impedance and (b) VSWR.

narrow unit cell boxes in Fig. 1. It has been shown in [12] that several severe resonances will occur in single-polarized TSA arrays if the electrical contacts are not present. This effect is observed also in the dual-polarized arrays.

D. Element Width w

In [4], Wunsch showed that some of the H-plane anomalies of dual-polarized arrays like that of Fig. 1 can be predicted by considering a dielectric-filled rectangular cavity having dimensions of a single array element and enclosed by metal walls on all sides except the aperture. The dielectric thickness t is small so that no variations of the cavity field are allowed in that direction. If the aperture wall were enclosed by a magnetic conductor, (4) gives the resonant frequencies of such a cavity. The dominant $m = p = 1$ mode of (4) predicts the observed H-plane anomaly within about 10%

$$f_{\text{res}} = \frac{c_o}{2\sqrt{\varepsilon_r}} \sqrt{\left(\frac{m}{w}\right)^2 + \left(\frac{2p-1}{2d}\right)^2}. \tag{4}$$

To further this investigation, the element width w is varied from 1.7–2.15 cm in increments of 0.15 cm. The other parameters R, D_a, and L_s are fixed at 0.3 cm^{-1}, 1.0 cm, and 4.5 cm, respectively. The tapered slot width H is fixed at 1.7 cm. As the element width are reduced, the frequencies at which anomalies occur increase. The D-plane VSWR plots are displayed in Fig. 11 because it is easier to distinguish the frequency shift since the anomalies are not as severe as in the H-plane.

The discrepancies between the observed resonant frequency and that calculated using (4) varies between 6% and 12% in line with the observations in [4]. As noted by Wunsch, the greatest discrepancies occur for small values of w, where the TSA slot removes a larger fraction of metal that comprises the "cavity" wall, thus having a greater impact on its resonant frequencies. By considering the two lowest order modes in (4), the H-plane anomalies can be predicted quite accurately. A study on these cavity resonances and the use of vias to control or eliminate them is reported in [11].

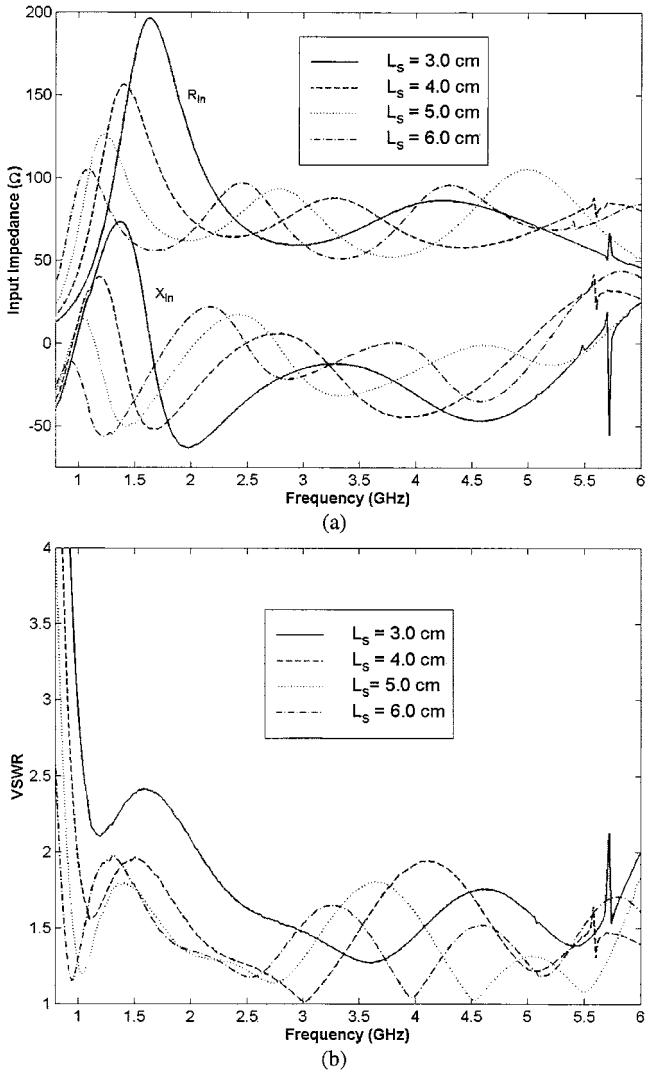

Fig. 10. Effects of tapered slotline length at broadside scan on (a) scan input impedance and (b) VSWR.

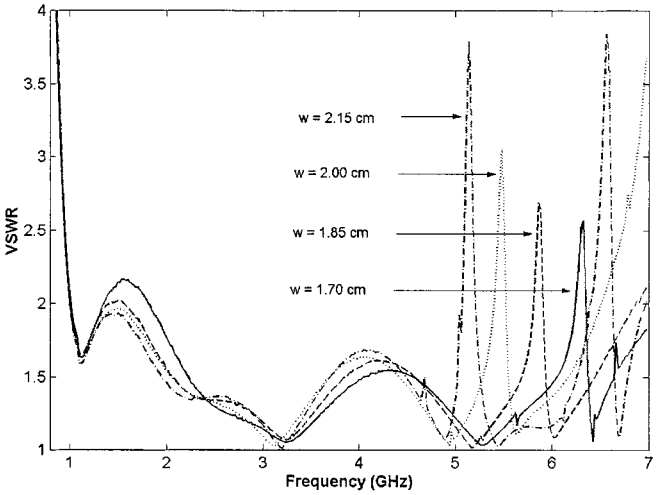

Fig. 11. D-plane scan $\theta = 45°$; effects of element width w on the onset of anomaly.

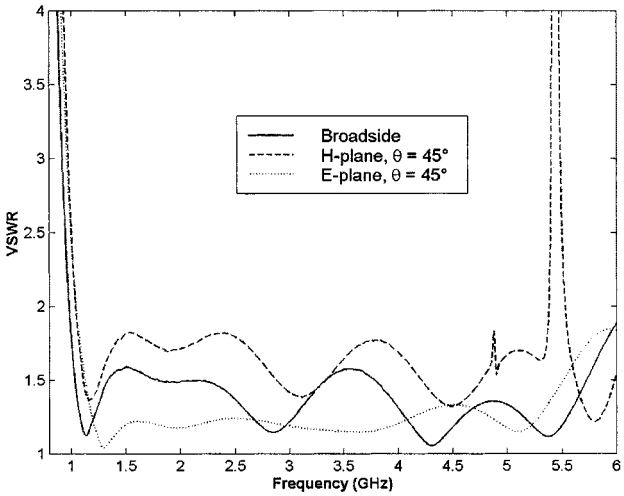

Fig. 12. Performance of design example for broadside E- and H-plane beam locations.

E. A Design Example

The use of data presented above to achieve a good design is illustrated through an example. The objective is to design an array that has VSWR < 2 for a scanning volume of not less than 45° from broadside in all planes while maintaining a large operating bandwidth. As a starting point, the opening rate is selected to be $R = 0.3$ cm^{-1} so that a relatively uniform in-band performance can be achieved. Choosing $w = 2$ cm limits f_U to around 4.9 GHz because of an H-plane anomaly. Recall that decreasing D_a reduces the first in-band hump at around 1.5 GHz and the mid-band hump at around 4 GHz, but at the expense of increasing f_L especially for H-plane scans. From Section III-C, increasing the length of the tapered slotline lowers f_L, but the VSWR hump at 1.5 GHz exceeds the VSWR < 2 criteria at the edge of the scan volume in the H-plane. Furthermore, the mid-band humps between 3 and 5 GHz occur at different frequencies for small D_a and long L_s and, therefore, compensate for each other. Thus, judicious choices of D_a and L_s may be able to achieve an optimized result.

After a limited amount of numerical "cut and try," optimum values $D_a = 0.85$ cm and $L_s = 5.5$ cm were chosen. The results are plotted in Fig. 12, which shows the VSWR performance for broadside beam angle as well as $\theta = 45°$ in the E- and H-planes. This choice of parameters combines in a way that the adverse effects of one parameter are compensated by another. The design has a bandwidth of about 4.5 : 1 and a scan volume not less than 45° from broadside in all planes with VSWR < 2. The antenna is lossless, i.e., no absorbers are used to dampen array or element resonances, so it is very efficient.

IV. Summary

Using a full-wave MoM analysis program with frequency interpolation of the MoM impedance matrix, a fairly comprehensive parameter study of dual-polarized TSA arrays was performed. It has been found that the key parameters that affect the bandwidth and scan performance of such arrays are the size of the slotline cavity, the length of the tapered slotline and the opening rate of the exponential taper. When the array is scanned

from broadside, the E-plane performance improves while the H-plane performance degrades. Furthermore, there are anomalies in the H-plane that are related to the element width and are probably caused by exciting cavity modes in the elements. Since the performance in the other scan planes is somewhat like a weighted average of the performance in the cardinal scan planes, the limitation of such an array is the H-plane scan. A study to control or eliminate the H-plane anomalies is underway.

Using data obtained from the parameter study, a design example using VSWR < 2 as a criteria, is shown to have about $4.5:1$ bandwidth and scan volume of not less than 45° in all scan planes. The design example illustrates that one can choose a particular parameter with good performance in a subband to mitigate another that degrades performance in that subband. This means that an antenna designer can use the parameter study as a guide to systematically design a wide-band widescan dual-polarized TSA array.

REFERENCES

[1] L. R. Lewis, M. Fasset, and J. Hunt, "A broad-band stripline array element," in *IEEE Int. Symp. Antennas Propagat. Dig.*, 1974, pp. 335–337.

[2] J. Shin and D. H. Schaubert, "Toward a better understanding of wide-band Vivaldi notch antenna arrays," in *Proc. Antenna Applicat. Symp.*, Monticello, IL, Sept. 1995.

[3] ——, "Parameter study of stripline-fed Vivaldi notch antenna arrays," *IEEE Trans. Antennas Propagat.*, vol. 47, pp. 879–886, May 1999.

[4] G. J. Wunsch, "Radiation characteristics of dual-polarized notch antenna arrays," Ph.D., Elect. Comput. Eng., Univ. Massachusetts, Amherst, Feb. 1997.

[5] H. Holter, , private communication.

[6] E. W. Lucas and T. P. Fontana, "A 3-D hybrid finite-element/boundary element method for unified radiation and scattering analysis of general infinite periodic arrays," *IEEE Trans. Antennas Propagat.*, vol. 43, pp. 145–153, Feb. 1995.

[7] D. T. McGrath and V. P. Pyati, "Phased-array antenna analysis with the hybrid finite element method," *IEEE Trans. Antennas Propagat.*, vol. 42, pp. 1625–1630, Dec. 1994.

[8] T.-H. Chio, "Finite element analysis of infinite phased array problems," Masters, Elect. Comput. Eng., Univ. Massachusetts, Amherst, Feb. 1997.

[9] E. H. Newman, "Generation of wide-band data from the method of moments by interpolating the impedance matrix," *IEEE Trans. Antennas Propagat.*, vol. 36, pp. 1820–1824, Dec. 1988.

[10] T.-H. Chio and D. H. Schaubert, "Effects of slotline cavity on dual-polarized tapered slot antenna arrays," in *IEEE Antennas Propagat. Soc. Int. Symp. Dig.*, Orlando, FL, July 1999, pp. 130–133.

[11] H. Holter, T.-H. Chio, and D. H. Schaubert, "Elimination of impedance anomalies in single- and dual-polarized endfire tapered slot phased arrays," *IEEE Trans. Antennas Propagat.*, vol. 48, pp. 122–124, Jan. 2000.

[12] D. H. Schaubert, "A gap-induced element resonance in single polarized arrays of notch antennas," *IEEE Antennas Propagat. Soc. Int. Symp. Dig.*, pp. 1264–1267, 1994.

Tan-Huat Chio received the B.Eng. (honors) from the National University of Singapore, in 1990, and the M.S.E.C.E. and Ph.D. degrees from the University of Massachusetts at Amherst, in 1997 and 1999, respectively.

From 1990 to 1993, he worked in the Defence Materiel Organization, Singapore. He is currently working in the DSO National Laboratories, Singapore. His research interests include printed antennas and wide-band phased arrays.

Daniel H. Schaubert (S'68–M'74–SM'79–F'89) has been at the University of Massachusetts at Amherst since 1982 and is currently a Professor of electrical and computer engineering. Prior to joining the faculty at the University of Massachusetts, he was Lead Scientist for the analysis of electromagnetic problems at the National Center for Devices and Radiological Health, Rockville, MD. He was also a Research Engineer at the Harry Diamond Laboratories near Washington, DC. He was coeditor (with D. Pozar) of *Microstrip Antennas* (Piscataway, NJ: IEEE Press, 1995).

Dr. Schaubert has been active in the IEEE Antennas and Propagation Society including serving as President, Vice President, two terms on the Administrative Committee, Secretary-Treasurer, Newsletter Editor, Distinguished Lecturer Program Coordinator, Associate Editor of TRANSACTIONS ON ANTENNAS AND PROPAGATION, and chapter offices in Washington, DC. He has worked with the organizing committees of the IEEE AP-S annual symposiums and he organizes the annual Antenna Applications Symposium.